A Novel Sampling Scheme for Text- and Image-Conditional Image Synthesis in Quantized Latent Spaces

Dominic Rampas[§]
Technische Hochschule Ingolstadt
Ingolstadt, Germany
and
Wand Technologies Inc.
New York, USA
dominic.rampas@gmail.com

Pablo Pernias[§]
Independent Researcher
Sant Joan d'Alacant, Spain
pablo@pernias.com

Marc Aubreville
Technische Hochschule Ingolstadt
Ingolstadt, Germany
marc.aubreville@thi.de

Abstract

Recent advancements in the domain of text-to-image synthesis have culminated in a multitude of enhancements pertaining to quality, fidelity, and diversity. Contemporary techniques enable the generation of highly intricate visuals which rapidly approach near-photorealistic quality. Nevertheless, as progress is achieved, the complexity of these methodologies increases, consequently intensifying the comprehension barrier between individuals within the field and those external to it. In an endeavor to mitigate this disparity, we propose a streamlined approach for text-to-image generation, which encompasses both the training paradigm and the sampling process. Despite its remarkable simplicity, our method yields aesthetically pleasing images with few sampling iterations, allows for intriguing ways for conditioning the model, and imparts advantages absent in state-of-the-art techniques. To demonstrate the efficacy of this approach in achieving outcomes comparable to existing works, we have trained a one-billion parameter text-conditional model, which we refer to as "Paella". In the interest of fostering future exploration in this field, we have made our source code and models publicly accessible for the research community.

1 Introduction

Recent advancements in the field of text-to-image synthesis [Gafni et al., 2022, Ramesh et al., 2022, Saharia et al., 2022, Rombach et al., 2022, Chang et al., 2023] have demonstrated substantial progress, as evidenced by the augmented diversity, enhanced quality, and the increased variation of generated images. At present, the majority of cutting-edge methodologies in this area primarily utilize either diffusion-based models [Ho et al., 2020, Saharia et al., 2022, Ramesh et al., 2022] or adopt transformer[Vaswani et al., 2017]-based architectures [Chang et al., 2023]. Although diffusion models achieve remarkable fidelity these outputs come with a heightened computational demand due to numerous sampling iterations and the amplifying complexity resulting from the application of increasingly sophisticated techniques. This intensification can lead to decreased inference speeds,
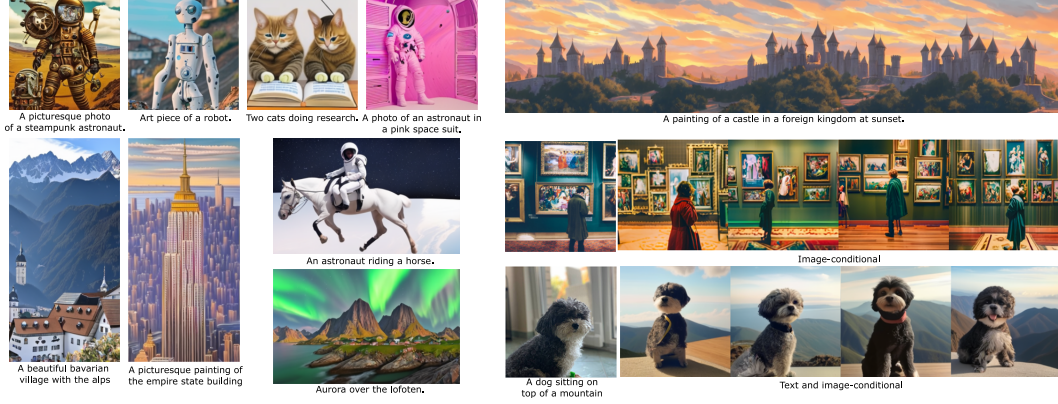
Figure 1: Visual results of our proposed method and trained model. It is able to perform a variety of image synthesis tasks. The left hand side and the top right shows our model's abilities on text-conditional image generation on different sizes while the two bottom right panels show image- and combined text and image-conditioning.
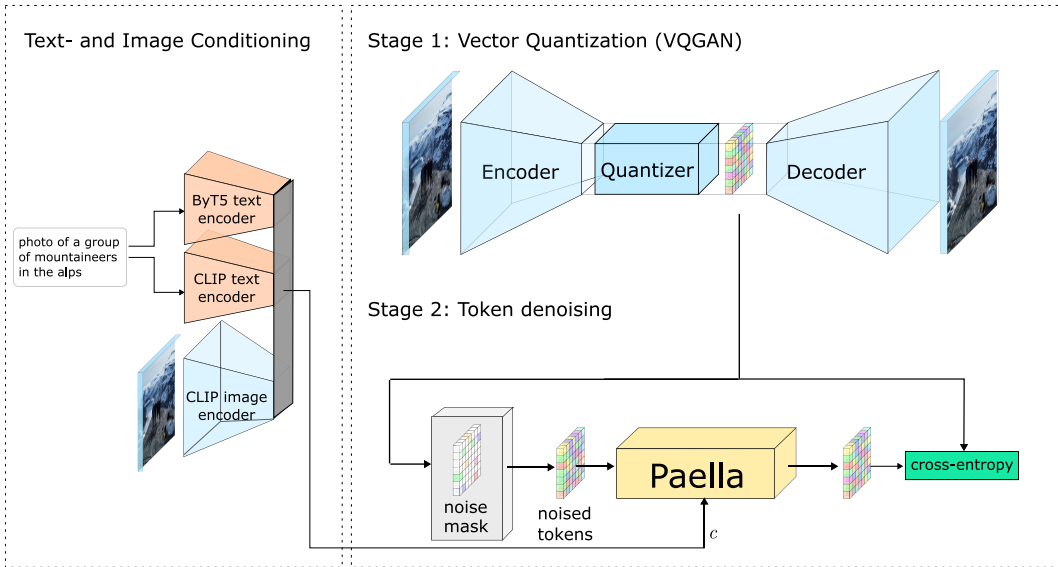

Figure 2: Visual depiction of the overall architecture of our proposed method. Training of *Paella* operates on a compressed latent space. Latent images are noised and the model is optimized to predict the unnoised version of the image.

rendering real-time implementation in end-user applications impractical. Further, it contributes to an elevated level of abstraction in comprehending the state-of-the-art technology, particularly for individuals outside of this specialized discipline. Although much work has been going into decreasing the number of sampling steps [Karras et al., 2022, Ho et al., 2020, Liu et al., 2022a], this stays an open problem and many large text-to-images models relying on diffusion are still using rather high numbers of steps. On the contrary, recent transformer-based approaches are able to use a much smaller number of inference steps, however employ a significant level of spatial compression, which can result in more artifacts but is necessary due to the self-attention mechanism growing quadratically with latent space dimensions. Furthermore, a transformer treats images as one-dimensional sequences by flattening the encoded image tokens, which is an unnatural projection of images and requires a significantly higher model complexity to learn an understanding of the 2D structure of images.

In this work, we propose a novel technique for text-conditional image generation, diverging from both transformer and diffusion-based approaches. Our model enables image sampling with remarkable efficiency, requiring as few as 12 steps while consistently producing high-fidelity results. Moreover,

the simplicity of our proposed technique enhances its accessibility, empowering individuals from various backgrounds to comprehend and implement this influential technology of text-to-image. Our proposed model uses a convolutional paradigm and functions within a discretized latent space, utilizing a Vector Quantized Generative Adversarial Network (VQGAN) [Esser et al., 2021] for both the encoding and decoding procedures (see Figure 2) at a modest compression rate. Given the convolutional characteristics of our model, we are capable of operating at significantly reduced compression rates, thereby circumventing conventional transformer constraints like quadratic memory expansion. Operating at a low compression rate facilitates the preservation of intricate details that are frequently altered in the context of higher compression scenarios. Throughout the training phase the quantized image tokens are noised by random token replacement. The model is subsequently tasked to reconstruct the image tokens, taking into account the noised variant and conditional input. The process of sampling new images unfolds iteratively and draws inspiration from methodologies employed by MaskGIT [Chang et al., 2022] and MUSE [Chang et al., 2023], but with significant changes: Both previous approaches incorporate a unique mask token and employ it to initially obscure the entire image. Subsequently, the model makes iterative predictions for all tokens in the image concurrently, retaining only a select number of tokens about which the model exhibits the highest confidence, while the remaining tokens are masked once more. We hypothesize this process to be inherently restrictive, as it precludes the model's capacity for self-correction of its early-stage predictions during sampling. To offer greater adaptability to the model, we randomly noise tokens as an alternative to masking them. This adjustment provides the model with the capability to refine its predictions for specific tokens throughout the sampling sequence. We enable text conditioning by using ByT5-XL [Xue et al., 2022] embeddings while additionally injecting pooled Contrastive Language-Image Pretraining (CLIP) [Radford et al., 2021] text-, and image embeddings intermittently. Owing to the convolution-based and spatially invariant nature of our token predictor, it possesses the capacity to generate images of any size, theoretically. In contrast, transformer-based models are required to incrementally adjust the context window to produce larger latent resolutions. Furthermore, as the model is conditioned in part on image embeddings, it affords the ability to generate variations of images in a zero-shot context and to combine images with supplementary text prompts. (Figure 6).

Our main contributions are the following:

1. We present an innovative convolution-based model for text- and image-conditional image generation, distinctly diverging from prevalent transformer and diffusion-based methods, thus providing a fresh viewpoint in the image generation field.

2. Our model demonstrates impressive efficiency, requiring only 12 steps for high-fidelity image generation, and is designed to enhance accessibility, democratizing the comprehension and implementation of this technology across diverse academic and professional spectra.

3. We introduce a novel approach for text-to-image sampling in quantized latent spaces, employing token renoising, which is deviating from traditional methods that rely on a special mask token. This enables iterative refinement of model predictions during the sampling sequence, thereby enhancing prediction accuracy.

4. We are publicly releasing the source code and the entire suite of model weights, all of which are licensed under the provisions of the MIT license.

2 Related Work

2.1 Conditional Image Generation

The field of text-conditional image generation has witnessed substantial advancements in recent periods. Initial explorations predominantly relied on Generative Adversarial Networks (GANs) [Reed et al., 2016, Zhang et al., 2017]. More recent methodologies have seen the emergence of a unique image generation framework known as diffusion [Sohl-Dickstein et al., 2015, Ho et al., 2020], which has not only achieved parity with GANs but has, in certain instances, surpassed them in both conditional and unconditional image generation [Dhariwal and Nichol, 2021]. Diffusion models propose a score-based architecture that iteratively purges noise from a target image, with the training objective articulated as a reweighted variational lower-bound. Recent investigations have demonstrated that diffusion models can be effectively scaled to high resolutions through multi-stage strategies, whilst preserving the capacity to generate high-fidelity images [Rombach et al., 2022, Saharia et al., 2022, Ramesh et al., 2022].

Recent advancements in image generation models [Rombach et al., 2022, Chang et al., 2023, Esser et al., 2021, Gafni et al., 2022, Ramesh et al., 2021, Ding et al., 2021] frequently employ a two-stage approach, wherein the initial stage involves encoding images into a more condensed latent space. The second stage encompasses learning within this compressed latent space, an approach that has proven to be more efficient for training a text-conditional model due to its lesser computational demands compared to pixel-level training. Initially, transformer-based models operated on an autoregressive basis, leading to a substantial deceleration in inference due to the necessity to individually sample each token. However, contemporary methodologies [Ding et al., 2022, Chang et al., 2022, Chang et al., 2023] have adopted the use of a bidirectional transformer to mitigate the limitations inherent in autoregressive models. Consequently, image generation can be achieved using a reduced number of steps, while simultaneously leveraging a global context during the generation process.

2.2 Conditional Guidance

Text conditional guidance of models is usually achieved by encoding text prompts with a pretrained language model. Two principal categories of text encoders are widely utilized: contrastive text encoders and uni-modal text encoders. CLIP [Radford et al., 2021], a contrastive multimodal model, endeavors to align semantically analogous textual descriptions and images within a unified latent space. Numerous recent approaches for image generation have relied on a frozen CLIP model as their sole method of conditioning. Dalle-2 by Ramesh *et al.* [Ramesh et al., 2022] only uses CLIP image embeddings as input to their diffusion model, while relying on a "prior" converting CLIP text embeddings to image embeddings. Stable Diffusion [Rombach et al., 2022] employs un-pooled CLIP text embeddings to condition its latent diffusion model [Rombach et al., 2022]. Contrastingly, works by Saharia *et al.* [Saharia et al., 2022], Liu *et al.* [Liu et al., 2022b] and Chang *et al.* [Chang et al., 2023] use a uni-modal large language model (T5 [Raffel et al., 2020] or ByT5 [Xue et al., 2022]) that can accurately encode textual prompts, resulting in more precise depictions regarding composition, style and layout.

3 Method

3.1 Training

Our proposal builds on the two-stage paradigm introduced by Esser *et al.* [Esser et al., 2021] and consists of a Vector-quantized Generative Adversarial Network (VQGAN) for projecting the high-dimensional images into a lower-dimensional latent space, as shown in Figure 2. Specifically, an encoder takes in the image at its base resolution of $H \times W \times C$ and maps it to a latent representation $\mathbf{u}$ with a resolution of $h \times w \times z$ with $h = H/f, w = W/f$, where f is the compression rate. This operation is followed by a quantization step, discretizing the latents by replacing each vector by its nearest neighbour from a learned codebook $Q \in \mathbb{R}^{N_{CB} \times z}$ of size N_{CB}. Afterwards, the quantized representation is given to the decoder which tries to reconstruct the input image. We use a pretrained VQGAN with an $f = 4$ compression and a base resolution of $256 \times 256 \times 3$, mapping the image to a latent resolution of 64×64 indices. The secondary phase involves learning the distribution of tokens within images situated in the low-dimensional latent space. During the training process, we introduce noise into the latent tokens derived from the encoded and quantized images by randomly substituting a certain proportion of the tokens with other randomly selected tokens from the codebook, as illustrated in Figure 3. The precise quantity of noised tokens is ascertained by randomly sampling from a uniform distribution ranging between 0 and 1, which the noising function interprets as the ratio of tokens to replace. Notice, we don't use a specific scheduling function to determine the ratio of tokens to noise as done in [Chang et al., 2022, Chang et al., 2023]. At training, a random number $t \sim \mathcal{U}(0, 1)$ is generated for each image. Subsequently, we sample a binary noise mask $\mathbf{m}$, with elements $m_{x,y}$, where a value of $m_{x,y} = 0$ indicates to keep the current token and a value of $m_{x,y} = 1$ signifies to noise it. The ratio of noised tokens is set to be equivalent to t. The noised tokens $\bar{u}_{x,y}$ at coordinate (x, y) are subsequently drawn from a uniform distribution $n_{x,y} \sim \mathcal{U}(0, N - 1)$ spanning all codebook indices:

$$\bar{u}_{x,y} = \begin{cases} u_{x,y} & \text{if} \quad m_{x,y} = 0 \\ n_{x,y} & \text{else} \end{cases}$$
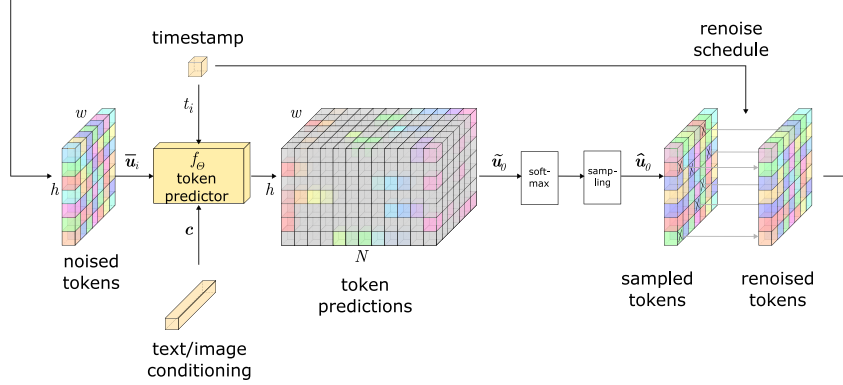
Figure 3: Sampling mechanism for the token predictor of our model.

The noised image representation, denoted as $\bar{u}$, is subsequently inputted into the token prediction model f_θ in conjunction with two additional parameters: the timestep t and a condition c. Mirroring the approach in diffusion models [Ho et al., 2020], we chose to incorporate the current timestep (noising ratio) into the model's input to provide an explicit information source concerning the amount of noise present within the image and the corresponding noise reduction expectation. While any condition can be included, such as class labels or semantic segmentation maps, we decided to condition the model on ByT5-XL [Xue et al., 2022] as the main source 95% of the time. Additionally, we also condition on CLIP [Radford et al., 2021] text-, and image-embeddings 5% of the time. The noised indices, the timestep embedding and the conditioning are given as input to the token predictor model which is tasked to predict the un-noised tokens, yielding a prediction $\tilde{\mathbf{u}} \in \mathbb{R}^{h \times w \times N_{CB}}$.

$$\tilde{\mathbf{u}} = f_\theta(\bar{\mathbf{u}}, \mathbf{c}, \mathbf{t})$$

The token predictor is optimized via cross-entropy using label smoothing. Preliminary experiments indicated that for small timesteps the model tended to emulate the identity function. We hypothesize that this was due to the already small loss, as a result of not many tokens being subjected to noising. This led to noisy samplings as the final iterations of noise removal were not adequately learned. To circumvent this problem, we introduced a loss weighting schedule that reduces the contribution to the loss of tokens that were not noised for smaller timesteps. The loss weighting is defined as follows:

$$l_w = 1 - (1 - m_{x,y}) \cdot ((1 - t) \cdot (1 - \eta))$$

We define η to be the minimum value a token can take for the loss contribution. We found $m_v = 0.3$ to yield satisfactory results.

Algorithm 1: Sampling function

Input : model $\mathbf{f}_\theta$, conditioning $\mathbf{c}$, latent shape s, sequence of noise ratios (timesteps) $t_1 > t_2 \cdots > t_T$, temperature τ, cfg-weight w, codebook size N_{CB}
Output : tokens to be decoded using the VQGAN decoder $\hat{\mathbf{u}}$

1 $\hat{\mathbf{u}}_{\text{init}} \leftarrow \text{randint}(\text{low} = 0, \text{high} = N_{CB}, \text{shape} = s)$;   /* Random initialization */
2 $\hat{\mathbf{u}} \leftarrow \hat{\mathbf{u}}_{\text{init}}$;
3 **for** $i = 1$ **to** T **do**
4      $\tilde{\mathbf{u}} \leftarrow \mathbf{f}_\theta(\hat{\mathbf{u}}, \mathbf{c}, t_i)$;   /* Single inference step */
5      $\tilde{\mathbf{u}} \leftarrow \tilde{\mathbf{u}} \cdot w + \mathbf{f}_\theta(\hat{\mathbf{u}}, \mathbf{c}_\emptyset, t_i) \cdot (1 - w)$;   /* CFG-weighting */
6      $\tilde{\mathbf{u}} \leftarrow \text{softmax}(\frac{\tilde{\mathbf{u}}}{\tau})$;
7      $\hat{\mathbf{u}} \leftarrow \text{multinomial}(\tilde{\mathbf{u}})$;   /* Token multinomial sampling */
8   **if** $i < T$ **then**
9         $\hat{\mathbf{u}} \leftarrow \text{renoise}(\hat{\mathbf{u}}, t_{i+1}, \mathbf{u}_{\text{init}})$;   /* Token renoising */
10   **end**
11 **end**

5

3.2 Sampling

While sampling in a single step would technically be possible, this procedure does not align properly with the training objective, as pointed out by [Chang et al., 2022]. Therefore, we are using an iterative approach for sampling too. Let $\mathbf{u}_T \in \mathbb{N}_0^{h \times w}$ be a latent image where each value is a random token from the codebook. Furthermore, let $\mathbf{t} = [t_1, t_2, \ldots, t_T]$ be the sequence of noising ratios at defined timesteps starting at $t_1 = 1$ (fully noised) and $t_T = 0$ (noise-free) with T being the number of sampling steps. Moreover, $\mathbf{c} \in \mathbb{R}^d$ denotes the conditional embedding. Sampling is conducted in an iterative fashion and the following steps are executed in each iteration:

1. The current noising ratio (time-step) $\mathbf{t}_i$, the latent space representation of the input $\mathbf{u}_i$, and the embedding $\mathbf{c}$ is given as input to the denoising model and it will predict all tokens simultaneously resulting in a score for each codebook index for the entire latent image. Specifically, after feeding an input $\mathbf{u}_i$, the output $\tilde{\mathbf{u}}_0$ has a shape of $h \times w \times N_{CB}$ where N_{CB} is the number of codebook vectors.

2. Afterwards a softmax function is applied to convert all scores to a probability distribution for each token in the latent image. Next, multinomial sampling is employed to sample one token from each distribution according to the probability. The result $\hat{\mathbf{u}}_0$ has a shape of $h \times w$.

3. We randomly renoise a certain proportion of all sampled tokens back to their initial noise codebook values $\hat{\mathbf{u}}_{\text{init}}$. This proportion is determined by the current noising ratio $\mathbf{t}_i$.

A visual depiction of the sampling algorithm can be seen in Figure 3 and the complete algorithm is given in Algorithm 1. Note that we renoise using the initial noise tokens instead of generating new random noise. We found this to lead to more robust outputs. Furthermore, unlike MaskGIT/MUSE we do not renoise the tokens with the lowest confidence and keep the ones with the highest scores, as this was not found to improve performance of our model. Instead, we renoised a random set of tokens for the sake of simplicity.

Additionally, we employed classifier-free-guidance (Classifier-Free Guidance (CFG)) [Ho and Salimans, 2022] for improving the sampling process. A null-label is introduced in the training. During sampling, we sample once with the null-label and once with the conditioning embedding. Afterwards we linearly interpolate between the logits (see line 5 in Algorithm 1).

3.3 Token Predictor Design Choices

Chang *et al.* use a bidirectional transformer for the image synthesis task. We argue that this implies two limiting factors: 1. Using a transformer necessitates treating the image as a flat 1D sequence, which is an unnatural projection of images and may impose a fundamental disadvantage during learning, since the 2D structure first needs to be learned through positional embeddings. 2. The quadratic memory growth limits transformers to small latent space resolutions, which in turn requires high compression rates. By replacing the transformer by a convolutional model, both aforementioned problems are resolved by having much lower memory requirements and induced 2D biases. Furthermore, we hypothesize the sampling strategy of MUSE/MaskGIT being too restrictive, as a token can not be changed after it has been fixed except by explicitly re-masking it, which prohibits the model to refine it's prediction at subsequent sampling iterations. Unfortunately, MUSE has no public release of the code & weights, making it hard to prove this hypothesis. To compensate this, we employed their sampling strategy and use the proposed confidence sampling, while fixing sampled tokens. A comparison between our proposed scheme and the aforementioned can be seen in Figure 4. An adjacent argument about the noising token can be made. Chang *et al.* use a unique mask token, about which we hypothesize is decreasing the diversity of outputs compared to using random tokens for the noising process. Denoising a specific masked image will always result in the exact same output logits. Diversity has to be forced during sampling, adding stochasticity through random sampling. On the contrary, our proposed sampling inherently encourages diversity through the initial noise. In Figure 4 we show that a single denoising step, starting from full noise, results in very different outcomes. In a model trained with mask tokens, this prediction would always be the same.

3.4 Token Predictor Architecture

Our architecture consists of a U-Net-style [Ronneberger et al., 2015] encoder-decoder structure based on residual blocks [He et al., 2016], employing convolutional and attention in both, the encoder and

Figure 4: a) Illustrative comparison between a single-step argmax denoising using masked tokens and random noise. The former (illustrated in the top row) always results in the same output, whereas random tokens give different outputs (bottom row), showing an intrinsic induced diversity in our method, while in a masked setting diversity needs to be induced in sampling. b) Comparison between low confidence renoising as used in MUSE (top) vs. our proposed random renoising (bottom).

the decoder path. The encoder and decoder consist of three levels. Attention blocks are only used at the two lowest levels to avoid memory overheads. To further increase the throughput, we use a patch size of 2 [Dosovitskiy et al., 2020, Liu et al., 2022c], which reduces the spatial dimensions while increasing the channels. This allows the model to scale flexibly to arbitrary latent dimensions. Besides the latent image, every block takes in the conditional embeddings and the timestep embedding. We use cross-attention [Vaswani et al., 2017] to combine the conditional embeddings with the image latents. Multiple conditionings from different models, ByT5 and CLIP [Xue et al., 2022, Radford et al., 2021], are first projected into a shared latent space and afterwards concatenated and propagated into the cross-attention layers. To enable the model with more capabilities to learn from the CLIP embeddings, the pooled embedding is projected into four separate embeddings, making room for learning different aspects in the individual heads.

4 Experiments

Prior to the training of the definitive model, we executed a series of scaled-down experiments to identify an appropriate and efficient architecture. This process involved training on reduced latent space dimensions, fewer model parameters, and smaller datasets. Subsequent to these preliminary investigations, we proceeded to train our comprehensive model, called *Paella*[1].

4.1 Training

We decided to use multiple models for conditioning and extract information from both text and images. The decision to use ByT5 [Xue et al., 2022] was due to recent investigations between character-aware and character-blind [Liu et al., 2022b] models, which concluded the former to be better at text rendering tasks. Additionally including CLIP text- and image-embeddings opened up many interesting downstream applications such as style-transfer, mixing multiple images, guiding text-conditional generation via images, image variations etc. Incorporating all previous findings and decisions, we trained our largest *Paella* model with 1B parameters. It was trained on 900 million images from the improved LAION-5B aesthetic [Schuhmann et al., 2022] dataset for $1M$ steps with a batch size of 2048. We further finetuned the model on a subset of the aesthetic dataset with aesthetic scores higher than six for $200k$ steps using a batch size of 1024. *Paella* uses a ByT5-XL encoder and a CLIP ViT-H/14 [Ilharco et al., 2021]. We trained on 128 NVIDIA A100 @ 80GB for three weeks. All experiments use AdamW [Loshchilov and Hutter, 2019] for optimization with a learning rate of $1e^{-4}$ using a linear warm-up schedule for 30k steps.

4.2 Text-Conditional Image Synthesis

To demonstrate *Paella's* text-conditional image generation capabilities we provide visual results (see Figure 1), but also quantitative numerical analysis (see Table 1). We evaluated zero-shot

---

[1]We named the model after the popular food paella, as in our initial experiments generating food always was the first thing to work well.
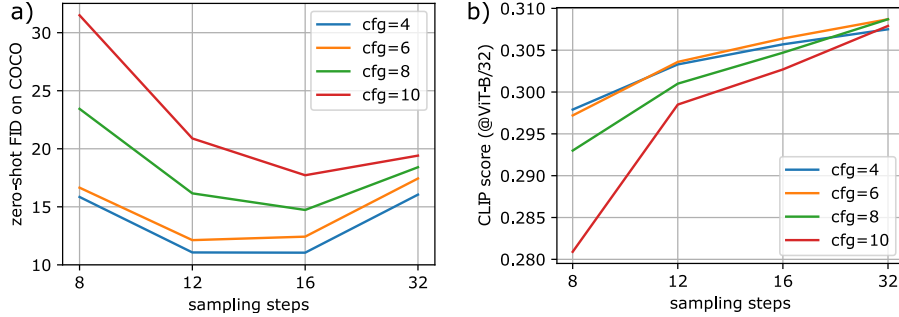
Figure 5: Dependency of the a) zero-shot Fréchet Inception Distance (FID) score [Heusel et al., 2017] and the b) CLIP score on the number of sampling steps.

Model	Parameters	Sampling Steps ↓	FID-COCO-30k ↓	open source	training data available
CogView [Ramesh et al., 2021]	4B	1024	27.1	✓	(partial)
Parti [Yu et al., 2022]	20B	1024	**7.23**	–	–
Make-A-Scene [Gafni et al., 2022]	4B	1024	11.84	–	(partial)
Imagen [Saharia et al., 2022]	2B	1000	7.27	–	–
DALL-E [Ramesh et al., 2021]	12B	256	17.89	–	–
DALL-E 2 [Ramesh et al., 2022]	3.5B	250	10.39	–	–
GLIDE [Nichol et al., 2021]	3.5B	250	12.24	–	–
LDM [Rombach et al., 2022]	0.4B	250	12.63	✓	✓
MUSE-3B [Chang et al., 2023]	3B	24	7.78	–	–
Paella (proposed)	1B	**12**	11.07	✓	✓

Table 1: Comparison of the zero-shot Fréchet Inception Distance to other state-of-the-art text-to-image methods on 256×256 images.

Fréchet Inception Distance (FID) [Heusel et al., 2017] scores to determine the faithfulness and fidelity compared to ground truth images from MS COCO [Chen et al., 2015]. Next to FID calculations, we assess the CLIP score between the captions and the generated images using CLIP ViT-B/32. We evaluate against different hyperparameter settings for the number of timesteps T and CFG weight w. The results can be found in Figure 5. We find the FID values to be highly competitive to state-of-the-art work as shown in Table 1, while having a fraction of the parameters, compared to most models, and using an order of magnitude fewer sampling iterations. Moreover, the CLIP score results show an increase in alignment with more sampling steps and that smaller CFG weights yield a better performance, especially for a lower number of iterations.

Figure 6: Image manipulation with Paella. a) shows image-conditional image generation, b) shows text-conditional image generation and c) shows image variations.

5   Discussion & Limitations

This work introduces an enhanced scheme for sampling in quantized latent spaces for text-to-image applications, allowing for a reduced number of sampling steps, while showing competitive fidelity, as

measured by the FID, to state-of-the-art works. As shown in Figure 5, the FID value of our model reaches its minimum for only 12 sampling steps, which in our view is a direct consequence of the novel sampling scheme, allowing for a higher diversity in the images, compared to the masking strategies employed by approaches such as MUSE or MaskGIT.

One interesting finding of our research is that our model is not particularly good at rendering text in images, which was reported by [Liu et al., 2022b] and was the main motivation for choosing ByT5 over T5. We link this possibly to an unintended consequence resulting from using quantized tokens, which only allows to either fully destroy or preserve information of a token. We leave this research question open for future investigation.

Another intriguing observation is that the model performance does not correlate positively with an increase in sampling steps regarding FID evaluations. Instead, it shows optimal performance at approximately 12 inference steps. This observation corroborates the findings of MaskGIT [Chang et al., 2022] and contradicts the conventional heuristic in diffusion models, where a higher number of sampling steps is typically associated with improved performance. However regarding the CLIP score, the model performs consistently better using more inference steps. This observation might indicate that fidelity emerges earlier than conditional alignment, showing that it is easier for the model to generate visually appealing images, than making them well aligned with the prompts. Contradicting to previous work as well, a higher CFG weight does not lead to an increase in the CLIP score for *Paella* and rather smaller guidance weights outperform higher ones on all timesteps.

6   Conclusion

In this work we presented *Paella*, a text- and image-conditional image generation system using a novel training objective and an improved sampling strategy. We showed that our model can generate high-fidelity images despite being smaller and requiring less steps for sampling than existing models, while still reaching competitive numerical results. We especially want to highlight the simple and straightforward setup of this model regarding training and sampling compared to models based on diffusion or transformers and believe this method will make generative techniques more accessible to a variety of people, even outside the research field of generative AI, which we argue will become crucial as this technology progresses further. We provide the final model weights and code on github [2]. Further, we provide training scripts and inference notebooks to support reproducibility of our findings.

References

[Chang et al., 2023] Chang, H. et al. (2023). Muse: Text-to-image generation via masked generative transformers. *arXiv:2301.00704*.

[Chang et al., 2022] Chang, H., Zhang, H., Jiang, L., Liu, C., and Freeman, W. T. (2022). MaskGIT: Masked generative image transformer. In *Proceedings of the IEEE/CVF Conference on Computer Vision and Pattern Recognition*, pages 11315–11325.

[Chen et al., 2015] Chen, X., Fang, H., Lin, T.-Y., Vedantam, R., Gupta, S., Dollár, P., and Zitnick, C. L. (2015). Microsoft COCO captions: Data collection and evaluation server. *arXiv:1504.00325*.

[Dhariwal and Nichol, 2021] Dhariwal, P. and Nichol, A. (2021). Diffusion models beat gans on image synthesis. *Advances in Neural Information Processing Systems*, 34:8780–8794.

[Ding et al., 2021] Ding, M., Yang, Z., Hong, W., Zheng, W., Zhou, C., Yin, D., Lin, J., Zou, X., Shao, Z., Yang, H., et al. (2021). Cogview: Mastering text-to-image generation via transformers. *Advances in Neural Information Processing Systems*, 34:19822–19835.

[Ding et al., 2022] Ding, M., Zheng, W., Hong, W., and Tang, J. (2022). Cogview2: Faster and better text-to-image generation via hierarchical transformers. *arXiv:2204.14217*.

[Dosovitskiy et al., 2020] Dosovitskiy, A., Beyer, L., Kolesnikov, A., Weissenborn, D., Zhai, X., Unterthiner, T., Dehghani, M., Minderer, M., Heigold, G., Gelly, S., et al. (2020). An image is worth 16x16 words: Transformers for image recognition at scale. In *Proceedings of the International Conference on Learning Representations (ICLR)*.

[Esser et al., 2021] Esser, P., Rombach, R., and Ommer, B. (2021). Taming transformers for high-resolution image synthesis. In *Proceedings of the IEEE/CVF Conference on Computer Vision and Pattern Recognition*, pages 12873–12883.

---

[2]`https://github.com/delicious-tasty/Paella`

[Gafni et al., 2022] Gafni, O., Polyak, A., Ashual, O., Sheynin, S., Parikh, D., and Taigman, Y. (2022). Make-a-scene: Scene-based text-to-image generation with human priors. *arXiv:2203.13131*.

[He et al., 2016] He, K., Zhang, X., Ren, S., and Sun, J. (2016). Deep residual learning for image recognition. In *Proceedings of the IEEE Conference on Computer Vision and Pattern Recognition*, pages 770–778.

[Heusel et al., 2017] Heusel, M., Ramsauer, H., Unterthiner, T., Nessler, B., and Hochreiter, S. (2017). GANs trained by a two time-scale update rule converge to a local nash equilibrium. *Advances in Neural Information Processing Systems*, 30.

[Ho et al., 2020] Ho, J., Jain, A., and Abbeel, P. (2020). Denoising diffusion probabilistic models. *Advances in Neural Information Processing Systems*, 33:6840–6851.

[Ho and Salimans, 2022] Ho, J. and Salimans, T. (2022). Classifier-free diffusion guidance. *arXiv:2207.12598*.

[Ilharco et al., 2021] Ilharco, G., Wortsman, M., Carlini, N., Taori, R., Dave, A., Shankar, V., Namkoong, H., Miller, J., Hajishirzi, H., Farhadi, A., and Schmidt, L. (2021). *OpenCLIP*. Zenodo.

[Karras et al., 2022] Karras, T., Aittala, M., Aila, T., and Laine, S. (2022). Elucidating the design space of diffusion-based generative models.

[Liu et al., 2022a] Liu, L., Ren, Y., Lin, Z., and Zhao, Z. (2022a). Pseudo numerical methods for diffusion models on manifolds. *arXiv:2202.09778*.

[Liu et al., 2022b] Liu, R., Garrette, D., Saharia, C., Chan, W., Roberts, A., Narang, S., Blok, I., Mical, R., Norouzi, M., and Constant, N. (2022b). Character-aware models improve visual text rendering. *arXiv:2212.10562*.

[Liu et al., 2022c] Liu, Z., Mao, H., Wu, C.-Y., Feichtenhofer, C., Darrell, T., and Xie, S. (2022c). A convnet for the 2020s. In *Proceedings of the IEEE/CVF Conference on Computer Vision and Pattern Recognition*, pages 11976–11986.

[Loshchilov and Hutter, 2019] Loshchilov, I. and Hutter, F. (2019). Decoupled weight decay regularization. *International Conference on Learning Representations (ICLR)*.

[Nichol et al., 2021] Nichol, A., Dhariwal, P., Ramesh, A., Shyam, P., Mishkin, P., McGrew, B., Sutskever, I., and Chen, M. (2021). Glide: Towards photorealistic image generation and editing with text-guided diffusion models. *arXiv:2112.10741*.

[Radford et al., 2021] Radford, A., Kim, J. W., Hallacy, C., Ramesh, A., Goh, G., Agarwal, S., Sastry, G., Askell, A., Mishkin, P., Clark, J., et al. (2021). Learning transferable visual models from natural language supervision. In *International Conference on Machine Learning*, pages 8748–8763. PMLR.

[Raffel et al., 2020] Raffel, C., Shazeer, N., Roberts, A., Lee, K., Narang, S., Matena, M., Zhou, Y., Li, W., Liu, P. J., et al. (2020). Exploring the limits of transfer learning with a unified text-to-text transformer. *J. Mach. Learn. Res.*, 21(140):1–67.

[Ramesh et al., 2022] Ramesh, A., Dhariwal, P., Nichol, A., Chu, C., and Chen, M. (2022). Hierarchical text-conditional image generation with CLIP latents. *arXiv:2204.06125*.

[Ramesh et al., 2021] Ramesh, A., Pavlov, M., Goh, G., Gray, S., Voss, C., Radford, A., Chen, M., and Sutskever, I. (2021). Zero-shot text-to-image generation. In *International Conference on Machine Learning*, pages 8821–8831. PMLR.

[Reed et al., 2016] Reed, S., Akata, Z., Yan, X., Logeswaran, L., Schiele, B., and Lee, H. (2016). Generative adversarial text to image synthesis. In *International conference on machine learning*, pages 1060–1069. PMLR.

[Rombach et al., 2022] Rombach, R., Blattmann, A., Lorenz, D., Esser, P., and Ommer, B. (2022). High-resolution image synthesis with latent diffusion models. In *Proceedings of the IEEE/CVF Conference on Computer Vision and Pattern Recognition*, pages 10684–10695.

[Ronneberger et al., 2015] Ronneberger, O., Fischer, P., and Brox, T. (2015). U-net: Convolutional networks for biomedical image segmentation. In *International Conference on Medical Image Computing and Computer-Assisted Intervention*, pages 234–241. Springer.

[Saharia et al., 2022] Saharia, C., Chan, W., Saxena, S., Li, L., Whang, J., Denton, E., Ghasemipour, S. K. S., Ayan, B. K., Mahdavi, S. S., Lopes, R. G., et al. (2022). Photorealistic text-to-image diffusion models with deep language understanding. *arXiv:2205.11487*.

[Schuhmann et al., 2022] Schuhmann, C., Beaumont, R., Vencu, R., Gordon, C., Wightman, R., Cherti, M., Coombes, T., Katta, A., Mullis, C., Wortsman, M., et al. (2022). Laion-5b: An open large-scale dataset for training next generation image-text models. *arXiv:2210.08402*.

[Sohl-Dickstein et al., 2015] Sohl-Dickstein, J., Weiss, E., Maheswaranathan, N., and Ganguli, S. (2015). Deep unsupervised learning using nonequilibrium thermodynamics. In *International Conference on Machine Learning*, pages 2256–2265. PMLR.

[Vaswani et al., 2017] Vaswani, A., Shazeer, N., Parmar, N., Uszkoreit, J., Jones, L., Gomez, A. N., Kaiser, Ł., and Polosukhin, I. (2017). Attention is all you need. *Advances in Neural Information Processing Systems*, 30.

[Xue et al., 2022] Xue, L., Barua, A., Constant, N., Al-Rfou, R., Narang, S., Kale, M., Roberts, A., and Raffel, C. (2022). Byt5: Towards a token-free future with pre-trained byte-to-byte models. *Transactions of the Association for Computational Linguistics*, 10:291–306.

[Yu et al., 2022] Yu, J., Xu, Y., Koh, J. Y., Luong, T., Baid, G., Wang, Z., Vasudevan, V., Ku, A., Yang, Y., Ayan, B. K., Hutchinson, B., Han, W., Parekh, Z., Li, X., Zhang, H., Baldridge, J., and Wu, Y. (2022). Scaling autoregressive models for content-rich text-to-image generation. *arXiv:2206.10789*.

[Zhang et al., 2017] Zhang, H., Xu, T., Li, H., Zhang, S., Wang, X., Huang, X., and Metaxas, D. N. (2017). Stackgan: Text to photo-realistic image synthesis with stacked generative adversarial networks. In *Proceedings of the IEEE international conference on computer vision*, pages 5907–5915.